J. Anat. (1999) **195**, pp. 359–373, with 9 figures Printed in the United Kingdom

Localisation and quantitation of autonomic innervation in the porcine heart II: endocardium, myocardium and epicardium

SIMON J. CRICK[1], ROBERT H. ANDERSON[1], SIEW YEN HO[1] AND MARY N. SHEPPARD[2]

[1] *Section of Paediatrics, National Heart & Lung Institute, Royal Brompton Campus, Imperial College of Science, Technology & Medicine, and* [2] *Department of Pathology, Royal Brompton Hospital, London, UK*

(*Accepted 18 May 1999*)

ABSTRACT

The immunological problems of pig hearts supporting life in human recipients have potentially been solved by transgenic technology. Nevertheless, other problems still remain. Autonomic innervation is important for the control of cardiac dynamics and there is evidence suggesting that some neurons remain intact after transplantation. Previous studies in the human heart have established regional differences in both general autonomic innervation and in its component neural subpopulations. Such studies are lacking in the pig heart. Quantitative immunohistochemical and histochemical techniques were used to demonstrate the pattern of innervation in pig hearts (*Sus scrofa*). Gradients of immunoreactivity for the general neural marker protein gene product 9.5 were observed both within and between the endocardial, myocardial and epicardial plexuses throughout the 4 cardiac chambers. An extensive ganglionated plexus was observed in the epicardial tissues and, to a lesser extent, in the myocardial tissues. The predominant neural subpopulation displayed acetylcholinesterase activity, throughout the endocardium, myocardium and epicardium. These nerves showed a right to left gradient in density in the endocardial plexus, which was not observed in either the myocardial or epicardial plexuses. A large proportion of nerves in the ganglionated plexus of the atrial epicardial tissues displayed AChE activity, together with their cell bodies. Tyrosine hydroxylase (TH)-immunoreactive nerves were the next most prominent subpopulation throughout the heart. TH-immunoreactive cell bodies were observed in the atrial ganglionated plexuses. Endocardial TH- and NPY-immunoreactive nerves also displayed a right to left gradient in density, whereas in the epicardial tissues they showed a ventricular to atrial gradient. Calcitonin gene-related peptide (CGRP)-immunoreactive nerves were the most abundant peptide-containing subpopulation after those possessing NPY immunoreactivity. They were most abundant in the epicardial tissues of the ventricles. Several important differences were observed between the innervation of the pig heart compared with the human heart. These differences may have implications for the function of donor transgenic pig hearts within human recipients.

Key words: Autonomic nervous system; intracardiac neurons; xenotransplantation.

INTRODUCTION

It is well known that the mammalian heart displays regionality in the distribution of autonomic innervation, whereby branches of sympathetic and parasympathetic nerves influence specific cardiac regions to a different extent (Mitrani & Zipes, 1994). Cardiac innervation is further complicated by the presence of intrinsic neurons, which are known to be capable of significant interaction with both efferent and afferent (sensory) neurons (Armour, 1994). The distribution of autonomic nerves within the endocardium, and throughout the myocardium, has been extensively investigated in the human heart using sensitive

Correspondence to Dr Simon J. Crick, Section of Paediatrics (Cardiac Morphology), National Heart & Lung Institute, Imperial College School of Medicine, Dovehouse Street, London, SW3 6LY, UK. Tel.: +44 (0) 171 352 8121, ext. 2253; fax: +44 (0) 171 351 8230; e-mail: s.crick@ic.ac.uk

immunohistochemical techniques (Wharton et al. 1990; Gordon et al. 1993*a*; Marron et al. 1994; Chow et al. 1995), and in the canine heart with the use of scintigraphic techniques (Dae et al. 1989, 1992). Such studies are lacking in the porcine heart. Electrophysiological properties of the atrial ganglionated plexus of the pig have suggested that porcine intrinsic neurons possess sympathetic as well as parasympathetic functional capabilities, and retain the ability to act independently when severed from their efferent inputs (Smith et al. 1992). This has also been observed in the acutely autotransplanted canine heart (Murphy et al. 1994). The study by Smith et al. (1992) also indicated that intrinsic neurons comprised an important contribution of the overall innervation of the pig heart. Nevertheless, anatomical evidence to support this contention is lacking. Furthermore, ventricular arrhythmias have been reported to occur in the regionally denervated porcine heart, indicating that regional differences are important in maintaining the normal function of the pig heart (Cinca et al. 1991). This may have potential implications for the development of harmful arrhythmias within the extrinsically denervated donor pig heart when placed in the human recipient. Knowledge of the extent and distribution of porcine cardiac innervation would prove useful for comparisons with other species, including man. It may also have possible implications for the functional dynamics of a donor transgenic pig heart within the human recipient.

The aims of this study, therefore, were to quantify and then compare the distribution of innervation and its neural subpopulations between the endocardial, myocardial and epicardial tissues of the 4 chambers of the pig heart.

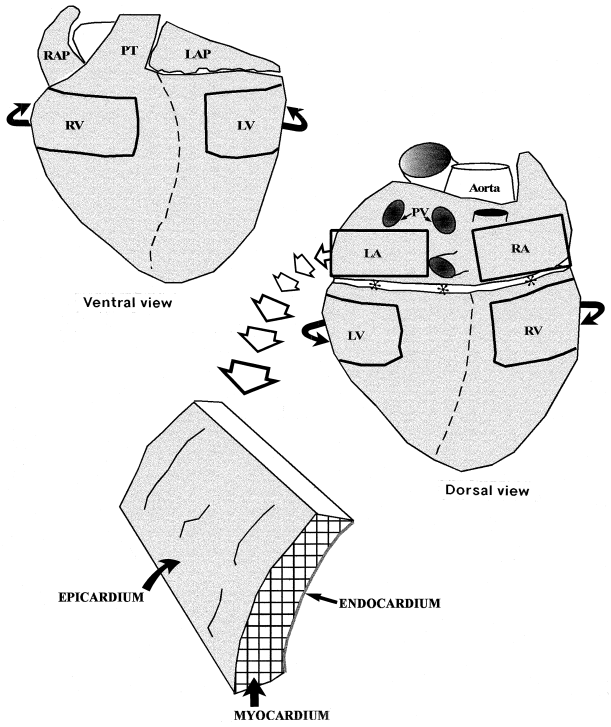

Fig. 1. Schematic diagrams showing ventral and dorsal aspects of the pig heart describing the sampling technique employed in the study for the collection of endocardial, myocardial and epicardial tissues. The endocardial and epicardial surfaces were dissected from the myocardium. Asterisks indicate location of the atrioventricular groove; RAP, right atrial appendage; PT, pulmonary trunk; LAP, left atrial appendage; RV, right ventricle; LV, left ventricle; PV, pulmonary veins; LA, left atrium; RA, right atrium.

MATERIALS AND METHODS

Tissue collection and processing

Fresh neonatal hearts were obtained from 10 piglets (*Sus scrofa*; age range 1–4 wk) killed by sodium pentobarbital injection. This procedure was in accordance with the Home Office Guidance on the Operation of the Animals (Scientific Procedures) Act 1986. Only piglet hearts were used in the study so that a greater extent of tissue could undergo analysis. Our previous study (see Crick et al. 1999, our accompanying article) and others (Gordon et al. 1993*a*; Chow et al. 1995) have reported that the innervation of the heart is intact at birth and changes in density are minimal during maturation. Hearts were excised within minutes of death and fixed by immersion in modified Bouin's solution for 16–24 h at 4 °C, as previously described (Crick et al. 1994). Each piglet heart was dissected so that the tissue blocks collected possessed directly comparable, but extensive, samples of endocardium, myocardium and epicardium (Fig. 1). The surface area of these tissue blocks was approximately 1–2 cm^2. The endocardial and epicardial surfaces were separated from the myocardium using fine dissection techniques under a Nikon SMZ-2T dissecting microscope, and then processed as whole mount preparations. The remaining myocardial tissue blocks were subsequently prepared for frozen sectioning. Briefly, these myocardial blocks were mounted on a cork mat, covered with Tissue-Tek mounting medium (Miles Inc., Elkhart, USA) and frozen in cooled isopentane suspended in liquid nitrogen. The blocks of myocardium underwent serial cryostat sectioning (15 μm) in the same plane as their endocardial and epicardial surfaces, that is in the same orientation as the majority of myocardial fibres. This ensured that the majority of nerve fibres and nerve trunks were sectioned in a similar plane to those of whole mount preparations from the endocardium

Table. *Source and characterisation of antisera*

Antigen	Species	Code	Dilution		Source
			Cryostat	Whole mounts	
PGP 9.5	Human	RA95	1:2000	1:1000	Ultraclone
TH	Bovine	TZ1010	1:400	1:400	Eugene Tech Int., USA
NPY	Synthetic peptide	951027B	1:200	1:200	Biogenesis Ltd.
CGRP	Rat	C-8198	1:1000	1:400	Sigma, UK
VIP	Mammalian	64-720	1:2000	1:400	ICN, UK
SOM	Mammalian	SZ1114	1:1000	1:400	Eugene Tech Int., USA

All primary antersera used were polyclonals raised from rabbit.

and epicardium. Variations in percentage stained nerve area caused by different orientation of nerve fibres would, therefore, potentially be eliminated during the image quantification procedure.

Immunostaining

An indirect immunofluorescence technique was adopted for the visualisation of innervation in both whole mount preparations and in cryostat sections. The technique for the immunofluorescent visualisation of innervation in cryostat sections of the myocardial blocks is described previously (see Crick et al. 1999). This procedure was modified for the immunofluorescent staining of whole mount preparations. Briefly, individual whole mounts were immersed in phosphate buffered saline containing 0.2% Triton X-100, washed in buffer and then stained with Pontamine sky blue. Whole mount preparations were then incubated for 16–24 h at room temperature in diluted primary antisera (see Table). Following washes in buffered saline, the preparations were incubated in fluorescein isothiocyanate (FITC) labelled goat antirabbit IgG (Dako, UK) at a dilution of 1:200. After further washes, the endocardial preparations were placed endothelial side up, and the epicardial preparations were placed mesothelial side up, on glass slides and mounted in Vectashield medium (Vector Laboratories, UK).

Acetylcholinesterase (AChE)-positive innervation was visualised in whole mount preparations using the method previously described for cryostat sections (see Crick et al. 1994, 1999). In control experiments, AChE activity was found to be absent following incubation of preparations without acetylthiocholine iodide and following the addition of 10^{-4} M eserine to the incubating solution.

The sequential visualisation of multiple neural subpopulations in whole mount preparations was achieved by the acid elution of antibody complexes using acidified potassium permanganate solution for up to 15 min (Marron et al. 1995). Briefly, previously photographed immunostained whole mount preparations were immersed in a solution containing 1 vol 2.5% $KMnO_4$, 1 vol 5% H_2SO_4, and 50 vol distilled water which denatures the antigen-antibody complex. The denaturation time was dependent on the thickness of the whole mount preparation and the avidity of the antibody for its antigen. After photography, the preparations were briefly destained in 0.5% disodium disulphite solution and washed several times in distilled water before incubation with the antiserum to the general neural marker PGP 9.5. The final stage in this sequential technique was the demonstration of AChE-positive innervation. Multiple sequential staining required careful control procedures. These included the reapplication of FITC-labelled goat antirabbit IgG after acid elution to confirm that denaturation was complete, and reapplication of the same or application of another neural marker following sequential visualisation of immunoreactivity to test that the morphology of nerve fibres had been unaffected by the treatment. Measurements of whole mount dimensions were made with an eyepiece graticule both before and after immunofluorescence and AChE staining procedures. No significant stretching or shrinkage of whole mounts was observed as a result of these procedures.

Quantification of innervation

Comparative quantitative data of the percentage stained nerve area of the overall pattern of innervation (PGP 9.5 immunoreactivity) and its individual neural subpopulations from the endocardium, myocardium and epicardium was obtained from all 4 chambers of

the pig heart. A similar image processing technique using the Quantimet 500+ system (Leica, Cambridge, UK) was adopted as previously employed for the analysis of the conduction system of the pig heart (see Crick et al. 1999). Both immunofluorescent and AChE-stained images were captured via a low-light colour video camera (JVC, model TK-1280E) mounted on a Leitz Laborlux S research microscope. The procedure for the quantification of innervation of whole mount preparations was the same as that previously described for cryostat sections (Crick et al. 1994). The process of interactive discrimination was standardised for each neural subpopulation undergoing analysis by adjusting the variable threshold level to a similar value for each measurement (within range ± 5 grey levels). Nerve fibres, small nerve bundles (fascicles) and nerve trunks were quantified although ganglion cells were excluded from these measurements. All fields of view covering the entire whole mount preparation and cryostat section were analysed, corresponding to approximately 30–40 fields per tissue sample. Measurements were taken from 5 serial cryostat sections from the myocardial blocks for each specific neural marker.

Statistics

The data are expressed as the mean and 95% confidence interval (95% CI) of the percentage stained nerve area, and are derived from the measurements taken from comparative regions of endocardium, myocardium and epicardium from all 4 chambers of 10 neonatal pig hearts. Following logit transformation of the data, the variation in the density of innervation between the endocardial, myocardial and epicardial tissues of the 4 chambers of the heart was assessed by analysis of variance. Differences with a P value of less than 5% were considered significant.

RESULTS

General pattern of innervation

The general distribution of nerves throughout selected regions of endocardium, myocardium and epicardium were assessed quantitatively by immunofluorescent staining for the general neural marker PGP 9.5. Endocardial innervation showed a gradient from right to left sides, with a significantly higher density of immunostained nerves being found in the right ventricular and right atrial endocardium compared with that of the left-sided chambers ($P < 0.0001$; Fig. 2). Myocardial innervation showed an atrial to ventricular gradient, with the significantly higher density of PGP 9.5-immunoreactive nerves in the myocardium of the right atrium, followed by the left atrium, and then the left and right ventricles, which possessed a similar, but much lower, density of nerves ($P < 0.0001$; Fig. 2). In contrast, the epicardial innervation showed a ventricular to atrial gradient in density of PGP 9.5-immunoreactive nerves, whereby the epicardium of both left and right ventricles displayed a higher percentage of immunostained nerve area than that of the right and left atria ($P < 0.0001$; Fig. 2). The complex neural network of these cardiac tissues was composed of numerous nerve trunks (diameter, 10–25 μm), together with varicose and nonvaricose nerve fibres (diameter 1–6 μm). Large nerve trunks were abundant within the epicardial plexus, especially in the epicardial tissue of the left ventricle (diameter, 40–160 μm). A proportion of epicardial nerve trunks was observed extruding from PGP 9.5-immunoreactive cardiac ganglia (Fig. 3). Itinerant subepicardial and subendocardial nerve trunks and fibres occasionally egressed these layers

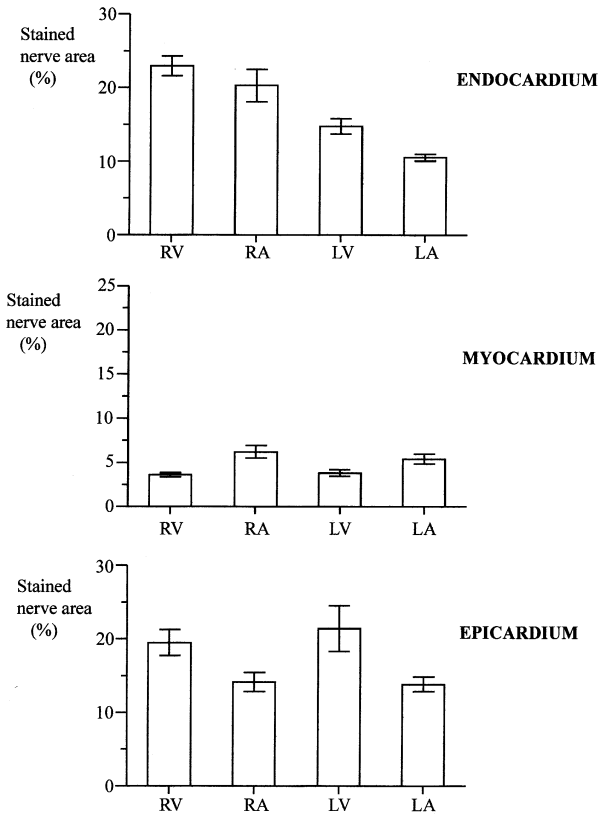

Fig. 2. Bar graphs showing distribution of percentage stained fluorescent nerve area of PGP 9.5-immunoreactive nerves throughout comparative regions of endocardial, myocardial and epicardial tissues. Each bar represents the mean and 95% confidence interval derived from 10 piglet hearts. RV, right ventricle; RA, right atrium; LV, left ventricle; LA, left atrium.

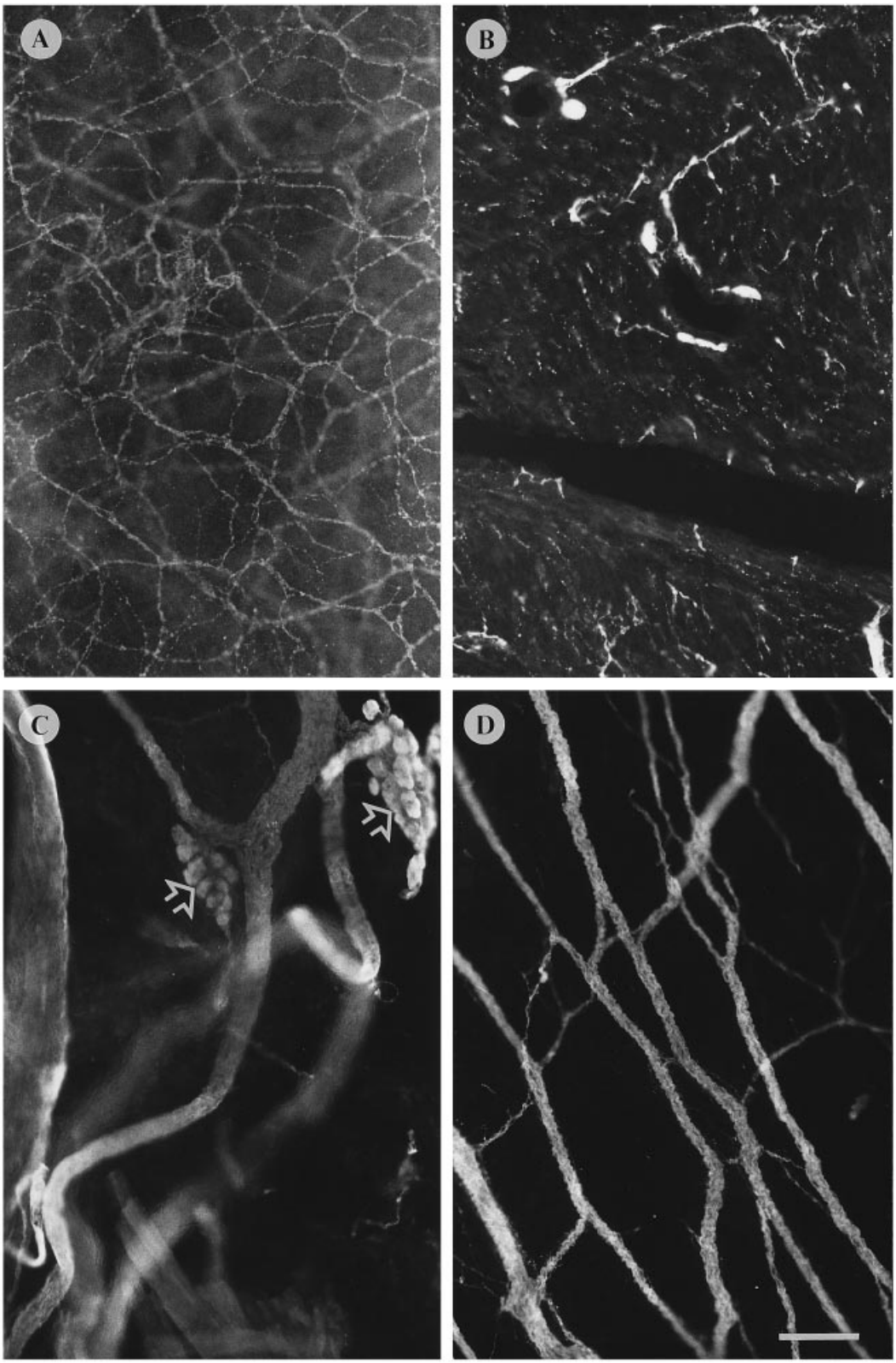

Fig. 3. Photomicrographs of PGP 9.5-immunoreactive innervation illustrating the comparative pattern of distribution in the endocardium (*A*), myocardium (*B*) and epicardium (*C*, *D*) of the right atrium. The neural plexus of the atrial epicardial tissues possess numerous ganglia (open arrows). Bar, 50 μm.

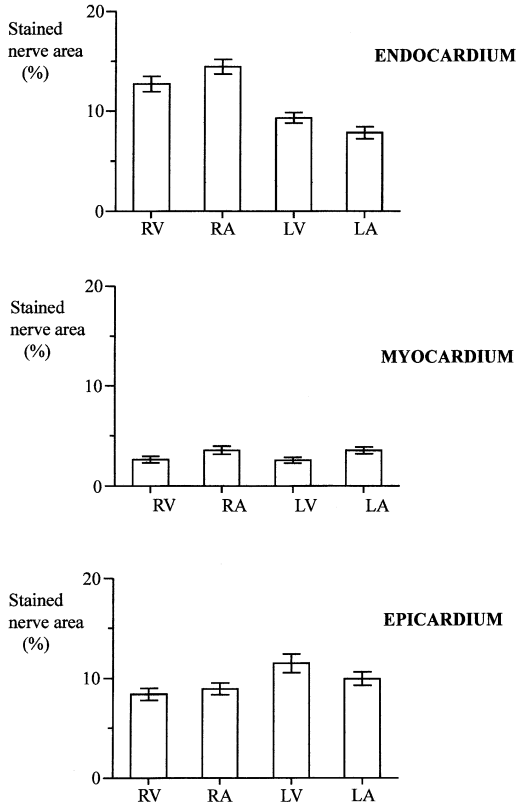

Fig. 4. Bar graphs showing distribution of percentage stained nerve area of AChE-positive nerves throughout comparative regions of the endocardial, myocardial and epicardial tissues. Each bar represents the mean and 95 % confidence interval derived from 10 piglet hearts. RV, right ventricle; RA, right atrium; LV, left ventricle; LA, left atrium.

and entered the underlying or overlying myocardium, respectively.

Distribution of neural subtypes

AChE-positive nerves were the predominant neural subtype observed throughout the endocardium, myocardium and epicardium (Fig. 4). The density and pattern of distribution of these nerves varied within as well as between the endocardial, myocardial and epicardial tissues, and also between the chambers of the heart (Fig. 5). AChE-positive nerves of the endocardial plexus displayed a right to left gradient in density which was absent from both the myocardial and epicardial tissues (Fig. 4). Nevertheless, endocardial AChE-positive nerves represented similar proportions of the total PGP 9.5-immunoreactive stained nerve area for the left (74 %) and right (71 %) atrial tissues. The endocardial tissues of the left and right ventricles possessed a significantly lower proportion of AChE-positive nerves and represented 63 % and 56 % of the total innervation, respectively ($P < 0.001$). There was, therefore, an atrial to ventricular

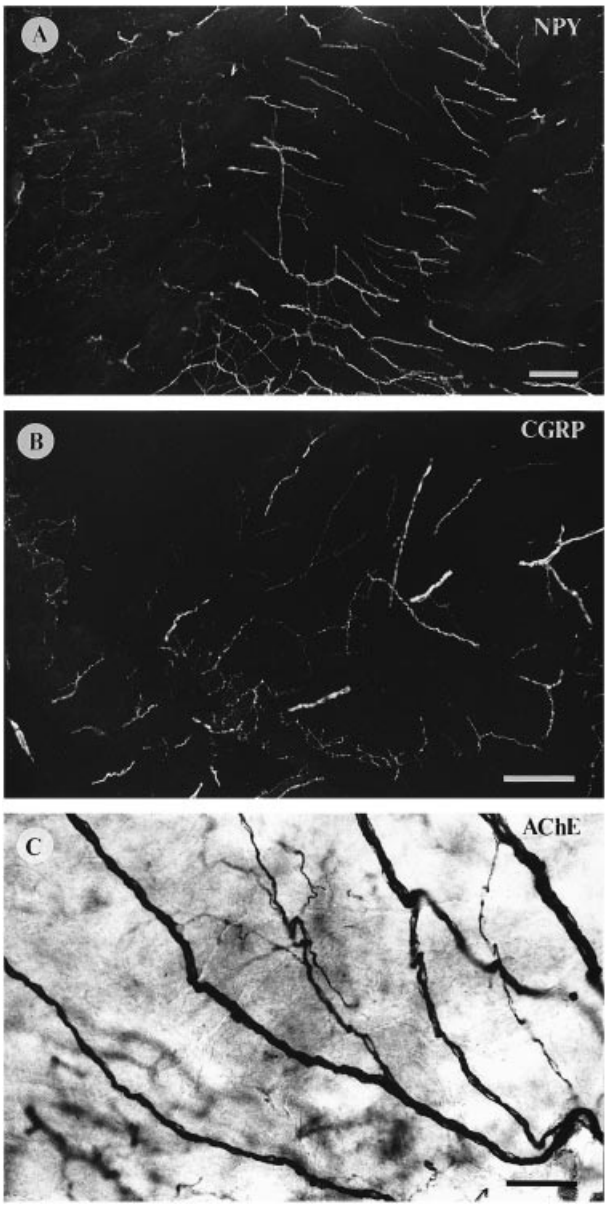

Fig. 5. Photomicrographs showing nerve fibres and fascicles immunoreactive for NPY (*A*) and CGRP (*B*) in the right atrial endocardium and nerves displaying activity for AChE in the right atrial epicardium (*C*). Bars, 50 μm.

gradient in AChE-positive nerves as a proportion of the total innervation, although both right and left ventricular endocardial tissues possessed a significantly higher relative density of these nerves than the endocardium of the left atrium ($P < 0.0001$; Fig. 4). There was no evidence of a density gradient of AChE-positive nerves between left and right sided chambers. In contrast, the myocardial tissues displayed a ventricular to atrial gradient in proportions of AChE-positive nerves. The largest proportion of total innervation was observed in the right ventricular myocardium (73 %), compared with the myocardial tissues of the left ventricle (67 %), left atrium (65 %)

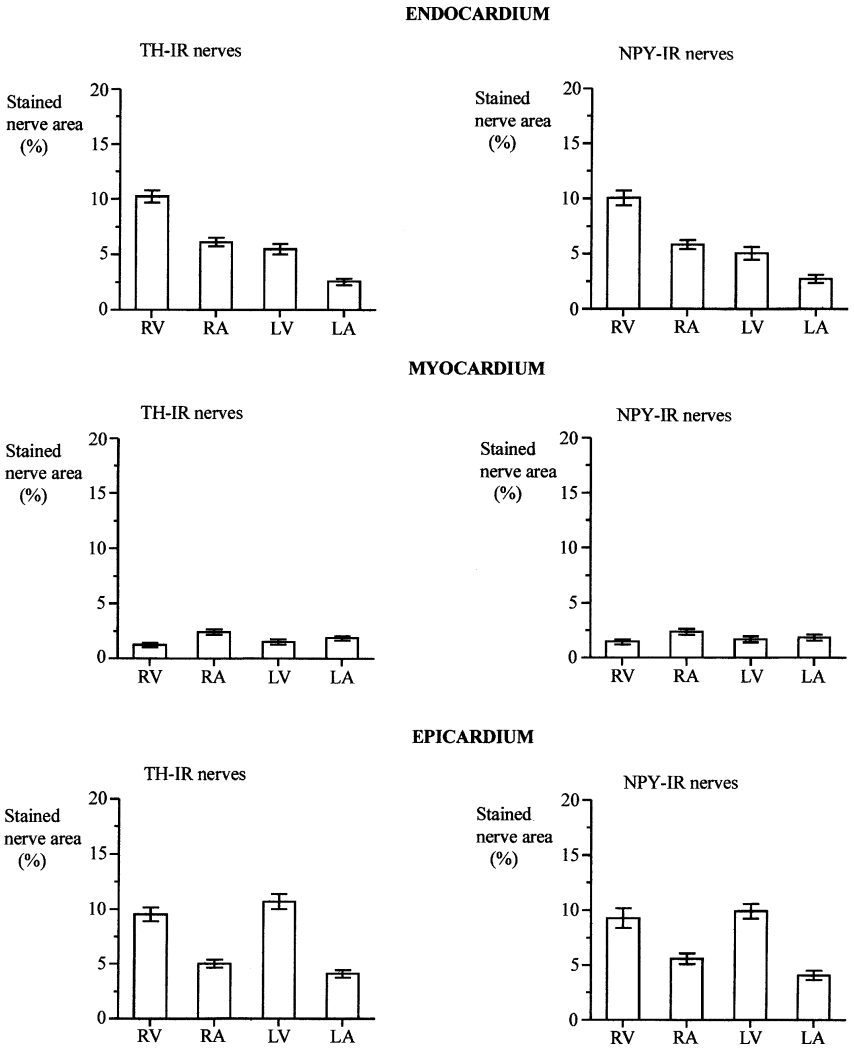

Fig. 6. Bar graphs showing distribution of percentage stained area of TH and NPY-immunoreactive nerves throughout comparative regions of the endocardial, myocardial and epicardial tissues. Each bar represents the mean and 95% confidence interval derived from 10 piglet hearts. RV, right ventricle; RA, right atrium; LV, left ventricle; LA, left atrium.

and right atrium (57%) (Fig. 4). Despite these relative proportions, the myocardium of the right and left atria possessed higher percentage stained area of AChE-positive nerves than the ventricular myocardium ($P < 0.0001$; Fig. 4). The epicardial tissues of the left ventricle possessed a significantly higher percentage stained area of AChE-positive nerves than the other 3 chambers ($P < 0.0001$). No significant difference was observed in the percentage stained area of these nerves between the left and right atrial epicardium ($P = 0.2760$), although a significantly lower value was observed in the right ventricular epicardial tissues ($P = 0.002$). AChE-positive nerves represented the highest proportion of the total pattern of innervation in the atrial epicardial tissues, the gradient being left atrium (72%), right atrium (63%), left ventricle (54%) and right ventricle (43%). A large proportion of the nerves in the ganglionated plexus of the atrial epicardial tissues displayed AChE activity, together with their cell bodies.

Nerves showing immunoreactivity for NPY represented the most numerous peptide containing subpopulation and displayed a similar density and distribution pattern to those nerves possessing TH immunoreactivity throughout the endocardial, myocardial and epicardial tissues (Fig. 6). Their distribution pattern was observed to be distinct from that of AChE-positive nerves following sequential staining techniques in whole-mount preparations (Fig. 7). A subpopulation of ganglion cell bodies in the atrial epicardial plexus, and particularly in the ganglia of the atrioventricular groove, demonstrated immunoreactivity for TH but did not display activity for AChE (Fig. 7). Endocardial TH and NPY-immunoreactive nerves also displayed a right to left gradient in density, whereas in the epicardial tissues they dis-

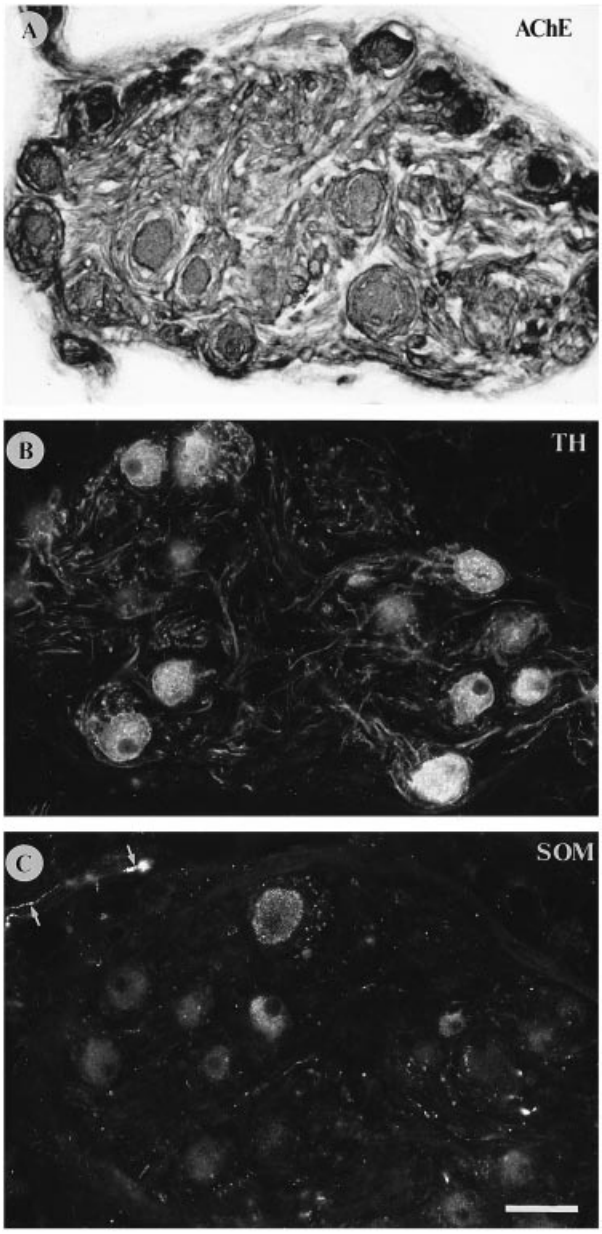

Fig. 7. Photomicrographs showing different patterns of localisation for AChE activity (*A*) and immunoreactivity for TH (*B*) and somatostatin (SOM; *C*) in cell bodies of the same intrinsic ganglion of the right atrial epicardial plexus. Many TH-immunoreactive nerve fibres are present around immunoreactive cell bodies (*B*). SOM-immunoreactive nerve fibres were also associated with immunoreactive cell bodies (small arrows). Bar, 50 μm.

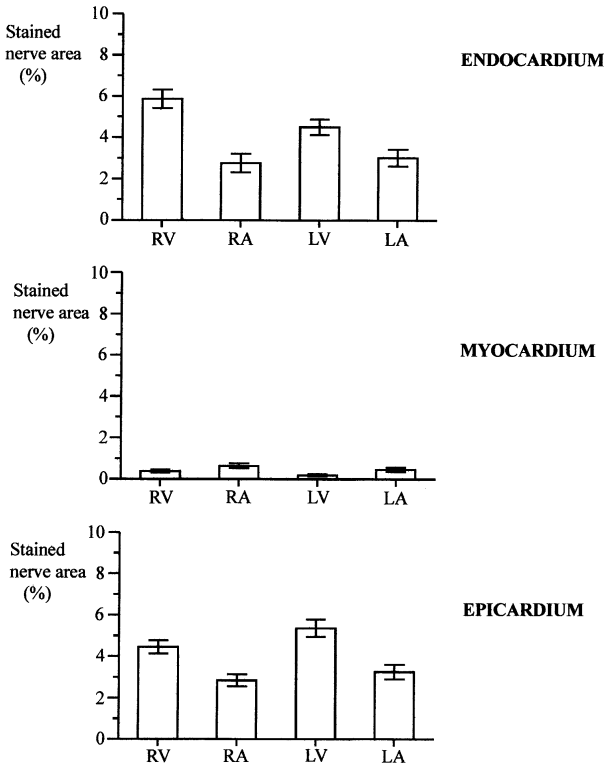

Fig. 8. Bar graphs showing distribution of percentage stained area of CGRP-immunoreactive nerves throughout comparative regions of the endocardial, myocardial and epicardial tissues. Each bar represents the mean and 95 % confidence interval derived from 10 piglet hearts. RV, right ventricle; RA, right atrium; LV, left ventricle; LA, left atrium.

played a ventricular to atrial gradient in density (Fig. 6). In the endocardial tissues, both these neural subtypes represented a higher proportion of the total PGP 9.5-immunoreactive nerve population in the right (45 %) and left (37 %) ventricles, compared with that of the right (30 %) and left (24 %) atrial chambers (Fig. 6). The right ventricular endocardium possessed a significantly higher percentage stained area of TH and NPY-immunoreactive nerves than the other chambers ($P < 0.0001$), but this was significantly lower than the percentage stained area of AChE-positive nerves observed in the same endocardial region ($P < 0.0001$). Similar proportions of TH and NPY-immunoreactive nerves were observed throughout the myocardial tissues, ranging from 35 to 40 % of the total innervation. Nevertheless, the right atrial myocardium possessed a significantly higher percentage stained area of these nerves than the left atrial, left ventricular and right ventricular myocardial tissues ($P < 0.0001$; Fig. 6). No significant difference was observed in the percentage stained area of TH-immunoreactive nerves in the myocardium of the left and right ventricles ($P = 0.506$; Fig. 6). Both these neural subtypes displayed a similar distribution in the epicardial tissues to that observed in the endocardium, with a ventricular to atrial gradient in the proportions of these nerves compared with the total PGP 9.5-innervation pattern. Approximately 49–50 % of the total innervation in the ventricular epicardial tissues was immunoreactive for TH and NPY, compared with 35 % and 30 % in the right and left atrial epicardial tissues, respectively. The ventricular epicardial tissues possessed an approximately 2-fold higher percentage stained area of these nerves com-

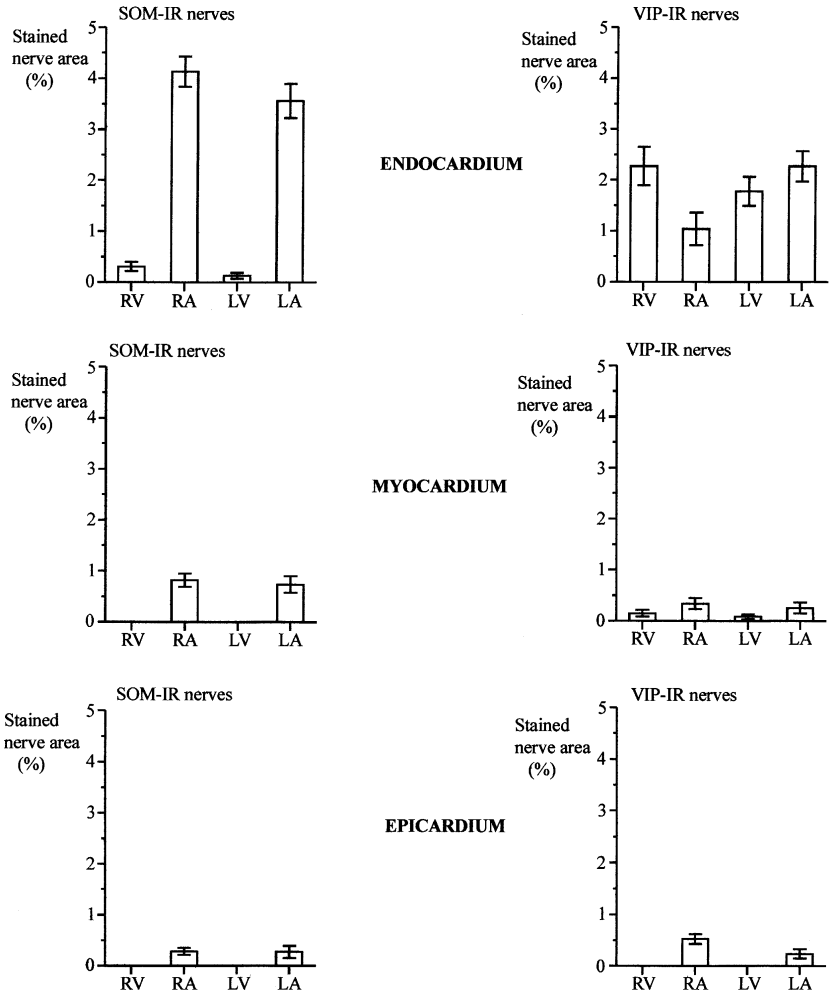

Fig. 9. Bar graphs showing distribution of percentage stained area of somatostatin (SOM) and VIP-immunoreactive nerves throughout comparative regions of the endocardial, myocardial and epicardial tissues. Each bar represents the mean and 95% confidence interval derived from 10 piglet hearts. RV, right ventricle; RA, right atrium; LV, left ventricle; LA, left atrium.

pared with that observed in the atrial epicardium ($P < 0.0001$; Fig. 6). No significant difference was observed in the relative density of TH-immunoreactive nerves between the endocardium and epicardium of the right ventricle ($P = 0.0878$), whereas the left ventricular epicardium possessed an approximately 2-fold higher density of these nerves compared with its endocardial surface ($P < 0.0001$; Fig. 6).

CGRP-immunoreactive nerves were the most abundant peptide-containing subpopulation observed after those possessing NPY immunoreactivity (Fig. 5). They possessed a distinct distribution compared with other neural subtypes. Nevertheless, some CGRP-immunoreactive varicose fibres were observed within predominantly AChE-positive nerve trunks, which themselves were often associated with epicardial coronary arteries. They were identified in the endocardium, myocardium and epicardium of all 4 chambers. A higher percentage stained area of these nerves was observed in the endocardium of the left and right ventricles compared with that of the atrial endocardium, with the highest value in the right endocardial tissues ($P < 0.0001$; Fig. 8). Nevertheless, CGRP-immunoreactive nerves represented 31% of the total PGP 9.5-immunoreactive nerve population in the left ventricular endocardium, 29% in the left atrial endocardium, with 26% and 14% observed in the right ventricular and right atrial endocardium, respectively. The distribution of CGRP-immunoreactive nerves also followed a left to right gradient in density in the myocardial tissues, although the relative proportions of these nerves compared with both the endocardial and epicardial tissues, was significantly lower ($P < 0.0001$; Fig. 8). In the myocardial tissues they represented approximately 10% of the total innervation in the right chambers, and 5–9% in the left chambers (Fig. 8). CGRP-immunoreactive nerves were most abundant in the epicardial tissues, representing 20–25% of the total innervation, with the epicardium of the left ventricle, left atrium and right ventricle possessing the larger relative proportions. The left ventricular epicardial tissues possessed a

significantly higher percentage stained area of CGRP-immunoreactive nerves compared with the other chambers ($P < 0.0001$), whereas in the endocardial tissues the highest value was observed in the right ventricular epicardium. Numerous CGRP-immunoreactive nerve fibres were present both within and around ganglion cell bodies of the atrial epicardial plexus, although the cell bodies themselves remained unreactive.

Somatostatin and VIP-immunoreactive nerves were the least abundant of neural subtypes identified. Nerves showing immunoreactivity for somatostatin were most abundant in the left and right atrial endocardium, where they represented approximately 34% and 20% of the total nerve population, respectively. They were also identified in the atrial myocardium, representing approximately 13% of the total innervation pattern in both left and right chambers. These nerves were sparse in atrial epicardial tissues, and completely absent from the myocardial and epicardial tissues of the ventricles (Fig. 9). Somatostatin-immunoreactive nerves displayed a different distribution pattern to that of NPY and TH-immunoreactive nerves, or those demonstrating AChE activity (Fig. 7). A number of somatostatin-immunoreactive cell bodies were also observed in the ganglionated plexus of both the left and right atrial epicardium (Fig. 7). VIP-immunoreactive nerves displayed a distinct pattern of distribution compared with all other neural subtypes. A proportion of VIP-immunoreactive nerve fibres in the left atrial endocardium were observed to be AChE-containing, but elsewhere no correlation was observed between their respective staining patterns. They were found to be most abundant in the endocardial tissues, especially in the left and right ventricles, and in the left atrium, representing 12%, 9% and 21% of the total nerve population, respectively (Fig. 9). Both the myocardial and epicardial tissues possessed a sparse distribution of these nerves (Fig. 9). No ganglion cell bodies within the epicardial plexus were found to be immunoreactive for VIP, although immunoreactive fibres were observed in close association with them.

DISCUSSION

This study has demonstrated the differential distribution of autonomic innervation within the endocardial, myocardial and epicardial tissues throughout the 4 chambers of the porcine heart. The findings of the study show that both the endocardium and epicardium of the pig heart possess a dense plexus of mixed autonomic and presumptive sensory nerves, with an uneven distribution throughout these cardiac tissues. This differential pattern has been observed in other mammalian hearts, such as that of the dog (Zipes & Miyazaki, 1990), cow (Gordon et al. 1993*b*), guinea pig (Dickson et al. 1981; Brown et al. 1985) and man (Gordon et al. 1993*a*; Marron et al. 1994; Chow et al. 1995).

The distribution of the total innervation pattern was visualised using the general neural marker PGP 9.5. In the endocardial tissues, there was a distinct right to left chamber gradient, with the right ventricle possessing the highest density of nerves and the left atrium the lowest. This pattern was similar to that observed in the human endocardial plexus (Marron et al. 1994), but was different from the pattern of innervation observed in the porcine myocardial and epicardial tissues. The myocardial tissues of the pig, as in cattle (Gordon et al. 1993*b*) and in man (Wharton et al. 1990), displayed an atrial to ventricular gradient in total nerve density. In contrast, the distribution of PGP 9.5-immunoreactive nerves in the epicardial tissues displayed a ventricular to atrial gradient in density. The innervation pattern of the epicardial tissues was characterised by a ganglionated plexus, with the atrial ganglia being located mainly around the atriovenous junctions (especially the pulmonary venous fat pad), and the ganglia serving the ventricular epicardial tissues situated within the atrioventricular groove. This contrasting pattern of distribution between the atrial endocardial and epicardial plexuses indicates that the ganglionated plexus of the atrial epicardium may represent an independent intracardiac nervous system to that of the endocardium. Nevertheless, there is evidence that these 2 plexuses may become integrated with each other as they traverse the atrioventricular groove, as observed in the canine heart (Chilson et al. 1985). This would explain the increase in density of overall innervation observed in the ventricular epicardium compared with that of the atrial epicardial tissue. Nonetheless, it is important to note that the high density of innervation that accompanies the atrioventricular conduction tissues on its passage into the interventricular septum may account, in part, for a proportion of both epicardial and endocardial ventricular innervation (see Crick et al. 1999). This study did not observe any significant variation within the different layers of the myocardium (i.e. subepicardium, midmyocardium, subendocardium). This is not to say, however, that subtle differences in the pattern of innervation do not exist, although a more specific study would be required to examine the distribution of terminal innervation within these cellular layers. Recent evidence indicates

that myocytes within these myocardial layers, especially in the ventricular walls, possess different action potential characteristics (Balati et al. 1998). For example, a layer of cells in the midmyocardium (M cells) has been found to possess prolonged action potential durations as a reflection of different repolarising currents (Balati et al. 1998).

Varicose nerve fibres, as well as nerve trunks, were observed throughout the endocardial and epicardial plexuses. Varicose nerve fibres have been shown to be in close physical contact with their surrounding endothelial or mesothelial cells, respectively (Marron et al. 1994, 1995). The distance between them corresponds to that of the autonomic neuromuscular junction, where transmitters released from these nerve varicosities affect the physiology of smooth muscle cells (Burnstock, 1986; Brock & Cunane, 1992). Indeed, regulatory factors released by epicardial mesothelial cells are known to alter both cardiac neurotransmission (Miyazaki et al. 1990) and myocardial contractility (Appelgate & Little, 1994; Eid et al. 1994).

The extensive ganglionated plexus observed in both the atrial and ventricular epicardial tissues suggests that the pig heart is served by a dense intrinsic nerve supply. The electrophysiological properties of porcine intrinsic cardiac neurons are known to differ from those of extracardiac autonomic neurons (Smith et al. 1992). The study by Smith et al. (1992) concluded that the cardiac ganglionated plexus of the pig represents a distinct population of autonomic neurons that may be capable of intracardiac integration of efferent information to the heart. The present study provides immunohistochemical evidence that the intracardiac nervous system of the pig possesses not only an extensive system of intrinsic AChE-containing postganglionic nerves, but also a significant population of intracardiac ganglion cells possessing immunoreactivity for the catecholamine-synthesising enzyme TH and also for the peptide, somatostatin. TH-containing nerve fibres had previously been thought to be of efferent postganglionic sympathetic origin (Wharton et al. 1990). Nevertheless, many studies have supported the finding of this study, namely that populations of intracardiac neurons possess catecholamines (Moravec et al. 1986; Hassall & Burnstock, 1987; Gagliardi et al. 1988; Haass et al. 1989; Moravec & Moravec, 1989; Armour & Hopkins, 1990*a*, *b*; Gordon et al. 1993*a*, *b*; Crick et al. 1996).

With the exception of the epicardial tissues, the innervation of the endocardium and myocardium of the pig heart displayed a right to left gradient in density. Functional studies in the canine heart have demonstrated differences in the site of action between right and left- sided branches of both efferent vagal and sympathetic cardiac nerves, providing further evidence that the 4 chambers of the mammalian heart receive a differential autonomic nerve supply (Mitrani & Zipes, 1994). For example, right-sided vagal and sympathetic nerves have a greater effect on the sinus node and heart rate, whereas left-sided vagal and sympathetic nerves exert more effect on the atrioventricular node (Randall et al. 1983; Randall & Ardell, 1990). Evidence from electrophysiological (Randall, 1984; Boineau et al. 1984), scintigraphic (Dae et al. 1989, 1992), and immunohistochemical studies (Gulbenkian et al. 1987; Wharton et al. 1990; Gordon et al. 1993*b*; Marron et al. 1994; Chow et al. 1995), support the finding of the present study that there are specific regions within the heart where supply of one individual nerve subpopulation predominates.

In the porcine endocardial, myocardial, and atrial epicardial tissues, the predominant neural subpopulation was found to possess AChE activity. The endocardial plexus showed a right to left gradient in density of AChE-positive nerves whereas this was reversed in the epicardial plexus. In contrast, similar levels of these nerves were observed throughout the myocardial tissues of the 4 chambers. In the ventricular epicardial tissues, however, these nerves were found in similar densities to TH and NPY-immunoreactive nerves. This is in contrast to human endocardial innervation, where TH-containing nerves were found in abundance in the ventricular chambers relative to the density of those containing AChE (Marron et al. 1994). The presence of AChE-containing nerves in the extrinsically denervated human heart (Wharton et al. 1990), and the presence of AChE activity in the majority of intracardiac neurons in culture (Hassall et al. 1990), indicates that a large proportion of these nerves can be considered as intrinsic postganglionic nerves originating from intracardiac ganglia. It may follow, therefore, that the predominance of AChE-positive nerves in the tissues of the porcine heart could be a result of a more extensive intrinsic system in comparison with that of the human heart. Nevertheless, the specific contribution of intrinsic nerves to the overall innervation of the pig heart cannot be precisely assessed from this study. This can only be achieved by measuring the density of innervation following total extrinsic denervation either by transplantation or by total cryoablation, as recently described in the bovine heart (Gordon et al. 1993*b*). It is known that intact intrinsic cardiac ganglion neurons in beating canine hearts

respond to electrical stimulation from both parasympathetic and sympathetic efferent cardiac nerves, as well as to activation of afferent cardiac and pulmonary mechanoreceptors (Gagliardi et al. 1988; Armour & Hopkins, 1990*a*, *b*). Furthermore, in the pig heart these intrinsic neurons have been shown to display spontaneous activity after decentralisation from neural connections of the central nervous system (Smith et al. 1992). In extrinsically denervated canine atria, an enhanced acetylcholine release has been reported to be a result of intrinsic neural supersensitivity, providing further evidence for the presence of an intact and functional intracardiac neuronal system (Smith & Priola, 1989). In addition, both sympathetic and parasympathetic responses can be elicited in intact dog hearts by focal stimulation of intrinsic cardiac ganglia (Butler et al. 1990). This indicates that the intracardiac neuronal system is capable of independent regulation of the heart and there is even evidence that intracardiac neurons can mediate local reflexes (Gagliardi et al. 1988; Armour & Hopkins, 1990*b*; Murphy et al. 1994). This may have implications for the function of a donor pig heart following transplantation into a human recipient. If the intrinsic nervous system of the porcine heart is more extensive relative to that of the human heart then it may create problems for the control of heart rate and contractility.

After AChE-positive innervation, TH and NPY-immunoreactive nerves represented the next most abundant neural subtypes throughout the pig heart. NPY-immunoreactive nerves showed a similar distribution pattern and relative density to that of TH-immunoreactive nerves throughout the endocardial, epicardial and myocardial tissues. This pattern has been observed in the endocardial and myocardial innervation of the human (Wharton et al. 1990; Marron et al. 1994), bovine (Gordon et al. 1993*b*), and canine (Forsgren, 1989) heart. These nerves also displayed a right to left gradient in density in the endocardial plexus, which was similar to that of AChE-positive nerves. In contrast, to epicardial AChE-positive innervation, both TH and NPY-immunoreactive nerves displayed a ventricular to atrial gradient within the epicardial tissues. Despite this, the density of these nerves was never observed to surpass that of AChE-positive innervation in either of the cardiac tissues assessed. The human endocardial plexus is also known to possess a right to left gradient in density of these nerves, however, a ventricular to atrial gradient is also present (Marron et al. 1994). This latter pattern was not observed in the endocardial plexus of the pig but, interestingly, was instead displayed by the epicardial plexus. This could indicate that presumptive sympathetic nerves travel predominantly in the epicardial tissues of the ventricles rather than in the endocardial tissues. Nevertheless, the pattern of distribution of TH and NPY-immunoreactive nerves suggests that presumptive sympathetic innervation is not as prominent in the ventricles of the pig heart as it is in the human ventricles (Marron et al. 1994). The majority of TH and NPY-immunoreactive nerves are thought to represent efferent postganglionic sympathetic nerves (Dalsgaard et al. 1986; Wharton et al. 1990). Despite this, the present study observed TH immunoreactivity in a subpopulation of ganglion cell bodies of the epicardial plexus indicating that a proportion of TH-immunoreactive nerves may represent intrinsic neurons. A number of these cell bodies were observed in the ganglia of the atrioventricular groove which may indicate that a significant proportion of TH-immunoreactive nerves supplying the porcine ventricles could be intrinsic in origin.

A relatively high proportion of CGRP-immunoreactive nerves was observed in the epicardial tissues, especially of the ventricles. They were observed to have a distinct distribution pattern to other neural subtypes but were, nevertheless, found in nerve trunks that contained mostly AChE-positive axonal profiles. These nerve trunks were often in close contact with ventricular epicardial coronary arteries such as the left anterior descending artery. The finding that these nerves possessed a similar distribution to AChE-positive nerves is in agreement with their localisation to AChE-containing nerves in the human endocardial plexus (Marron et al. 1994). Nevertheless, the issue whether CGRP is colocalised with AChE in the same nerve fibres or is found in different axons running in close proximity was impossible to resolve in this study. CGRP has been found to be involved in porcine coronary vasodilation (Franco-Cereceda, 1991), and may also play a role in the neurally mediated negative inotropic effect on myocardial function observed during cholinergic coronary vasoconstriction in pigs (Cinca et al. 1996). CGRP-immunoreactive nerves are thought to be afferent in origin, arising from vagal or dorsal root sensory neurons (Wharton et al. 1990; Forsgren, 1994). Nonetheless, the demonstration of CGRP-containing nerves cannot be assumed to represent unequivocal evidence that these fibres are entirely sensory in function. There is evidence that CGRP is present in intrinsic neurons which are not considered to play an afferent role (Gerstheimer & Metz, 1986). CGRP is thought to be involved in the transmission of pain and is known to be colocalised with substance P (Wharton

et al. 1986). Furthermore, vagal afferent nerves are thought to be involved in the mediation of cardiac pain during coronary occlusion and ischaemia (Meller & Gebhart, 1992). Anginal pain has been relieved in a small number of patients by unilateral or bilateral vagotomy, where initial sympathetic denervation had no effect (Meller & Gebhart, 1992).

Both somatostatin and VIP-immunoreactive nerves were relatively sparse in comparison with other neural subtypes, and they both displayed distinct patterns of distribution. In contrast to the distribution of somatostatin in the human endocardial plexus, this study did not find a correlation between these nerves and those containing AChE (Marron et al. 1994). In the pig heart, somatostatin-immunoreactive cell bodies were observed in the ganglia of the atrial epicardial plexus, indicating that somatostatin is localised to intrinsic neurons. The function of these nerves in the porcine heart remains unclear. The peptide is known to play a role, nonetheless, in the modulation of atrial contractility and atrioventricular nodal conduction in the human heart (Day et al. 1985). VIP-immunoreactive nerves were predominantly observed in the endocardial plexus. They had a different distribution to other neural subtypes and no ganglion cell bodies were found to possess VIP immunoreactivity, indicating that they do not represent intrinsic neurons. In the human heart, these nerves are thought to represent postganglionic parasympathetic nerves (Wharton et al. 1990) but there is evidence that VIP-immunoreactive nerve fibres and cell bodies are colocalised with noradrenergic nerves in the thoracic sympathetic chain ganglia of the pig (Hill & Elde, 1989). This indicates that VIP may be localised to postganglionic sympathetic neurons in the porcine heart.

In summary, this study has described the quantitative distribution of autonomic innervation throughout the endocardial, myocardial and epicardial tissues of the porcine heart. Several important differences were observed between the innervation of these cardiac tissues in the pig compared with those of the human heart. Most importantly, the study has described the presence of an extensive intracardiac nerve system, which may be responsible for the higher density of AChE-positive nerves observed throughout the porcine heart compared with the human heart. It is important that we note the significance of this intrinsic system since there is electrophysiological evidence that it can operate independently of efferent innervation in the porcine heart (Smith et al. 1992). This may have potential implications for the function of a donor transgenic pig heart within the human transplant patient. Transgenic pig hearts have recently been transplanted into nonhuman primates (baboons) with ambiguous results (Schmoeckel et al. 1998). This study reported that a proportion of grafts failed within 18 h without any histological signs of hyperacute rejection. Some of the recipients died because of failure to produce even a low cardiac output and/or dysrhythmia. It is clear from this initial trial that more research is required into the optimum immunosuppressive regimen before any attempts are made into investigations of graft physiology. Nevertheless, the fact that a proportion of these grafts failed as a result of arrhythmogenic mechanisms, may or may not be significant in the light of our findings concerning the intrinsic nervous system of the heart. Further trials using the pig-to-primate model are essential.

ACKNOWLEDGEMENTS

This work was funded by a grant from the British Heart Foundation. The authors express their thanks to Dr Alison Hislop, Dr Joan Deutsch and Professor S. G. Haworth (Institute of Child Health, London, UK) for providing us with a number of neonatal pig hearts.

REFERENCES

APPELGATE RG, LITTLE WC (1994) Alteration of autonomic influence on left ventricular contractililty by epicardial superfusion with hexamethonium and procaine. *Cardiovascular Research* **28**, 1042–1048.

ARMOUR JA (1994) Peripheral autonomic neuronal interactions in cardiac regulation. In *Neurocardiology* (ed. Armour JA, Ardell JL), pp. 219–244. New York: Oxford University Press.

ARMOUR JA, HOPKINS DA (1990*a*) Activity of in vivo canine ventricular neurons. *American Journal of Physiology* **258** (2 Pt 2), H320–H336.

ARMOUR JA, HOPKINS DA (1990*b*) Activity of in situ canine left atrial neurons. *American Journal of Physiology* **259** (4 Pt 2), H1207–H1215.

BALATI B, VARRO A, PAPP JG (1998) Comparison of the cellular electrophysiological characteristics of canine left ventricular epicardium, M cells, endocardium and Purkinje fibres. *Acta Physiologica Scandinavica* **164**, 181–190.

BOINEAU JP, MILLER CB, SCHUESSLER RB, ROESKE WR, AUTRY LJ, WYLDS AC et al. (1984) Activation sequence and potential distribution maps demonstrating multicentric atrial impulse origin in dogs. *Circulation Research* **54**, 332–347.

BROCK JA, CUNNANE TC (1992) Electrophysiology of neuroeffector transmission in smooth muscle. In *Autonomic Neuroeffector Mechanisms* (ed. Burnstock G, Hoyle CHV), pp. 121–214. Chur, Switzerland: Harwood Academic.

BROWN OM, SALATA JJ, GRAZIANI LA (1985) The distribution of acetylcholine and choline in guinea pig heart. *Life Science* **36**, 383–389.

BURNSTOCK G (1986) Autonomic neurovascular junctions: current developments and future directions. *Journal of Anatomy* **146**, 1–30.

BUTLER CK, SMITH FM, CARDINAL R, MURPHY DA, HOPKINS DA, ARMOUR JA (1990) Cardiac responses to

electrical stimulation of discrete loci in canine atrial and ventricular ganglionated plexi. *American Journal of Physiology* **259**, H1365–H1373.

CINCA JF, WERNER A, BARDAJ A, SALAS-CAUDARILLA A, SOLER-SOLER J (1991) Induced ventricular arrhythmias in regionally denervated porcine heart with healed myocardial infarction. *Cardiovascular Research* **25**, 586–593.

CINCA J, CARRENO A, MONT L, BLANCH P, SOLER-SOLER J (1996) Neurally mediated negative inotropic effect impairs myocardial function during cholinergic coronary vasoconstriction in pigs. *Circulation* **94**, 1101–1108.

CHILSON DA, PEIGH P, MAHOMED Y, ZIPES DP (1985) Encircling endocardial incision interrupts efferent vagal-induced prolongation of endocardial and epicardial refractoriness in the dog. *Journal of the American College of Cardiology* **5**, 290–296.

CHOW LT, CHOW SS, ANDERSON RH, GOSLING JA (1995) The innervation of the human myocardium at birth. *Journal of Anatomy* **187**, 107–114.

CRICK SJ, WHARTON J, SHEPPARD MN, ROYSTON D, YACOUB MH, ANDERSON RH et al. (1994) Innervation of the human cardiac conduction system. A quantitative immunohistochemical and histochemical study. *Circulation* **89**, 1697–1708.

CRICK SJ, SHEPPARD MN, ANDERSON RH, POLAK JM, WHARTON J (1996) A quantitative assessment of innervation in the conduction system of the calf heart. *Anatomical Record* **245**, 685–698.

CRICK SJ, SHEPPARD MN, HO SY, ANDERSON RH (1999) Localization and quantitation of autonomic innervation in the porcine heart I: Conduction system. *Journal of Anatomy* **195**, 341–357.

DAE MW, O'CONNELL JW, BOTVINICK EH, AHEARN T, YEE E, HUBERTY JP et al. (1989) Scintigraphic assessment of regional cardiac adrenergic innervation. *Circulation* **79**, 634–644.

DAE MW, DEMARCO T, BOTVINICK EH, O'CONNELL JW, HELTNER RS, HUBERTY JP et al. (1992) Scintigraphic assessment of MIBG uptake in globally denervated human and canine hearts: implications for clinical studies. *Journal of Nuclear Medicine* **33**, 1444–1450.

DALSGAARD C-J, FRANCO-CERECEDA A, SARIA A, LUNDBERG JM, THEODORSSON-NORHEIM E, HÖKFELT T (1986) Distribution and origin of substance P- and neuropeptide Y-immunoreactive nerves in the guinea pig heart. *Cell and Tissue Research* **243**, 477–485.

DAY SM, GU J, POLAK JM, BLOOM SR (1985) Somatostatin in the human heart and comparison with guinea pig and rat heart. *British Heart Journal* **53**, 153–157.

DICKSON DW, LUND DD, SUBIETA AR, PRALL JL, SCHMID PG, ROSKOSKI R (1981) Regional distribution of tyrosine hydroxylase and dopamine beta-hydroxylase activities in guinea pig heart. *Journal of the Autonomic Nervous System* **4**, 319–326.

EID H, DE BOLD MLK, CHEN JH, DE BOLD AJ (1994) Epicardial mesothelial cells synthesize and release endothelin. *Journal of Cardiovascular Pharmacology* **24**, 715–720.

FORSGREN S (1989) Neuropeptide Y-like immunoreactivity in relation to the distribution of sympathetic nerve fibres in the heart conduction system. *Journal of Molecular & Cellular Cardiology* **21**, 279–290.

FORSGREN S (1994) Distribution of calcitonin gene-related immunoreactivity in the bovine conduction system: correlation with substance P. *Regulatory Peptides* **52**, 7–19.

FRANCO-CERECEDA A (1991) Resiniferatoxin-, capsaicin- and CGRP-evoked porcine coronary vasodilation is independent of EDRF mechanisms but antagonised by CGRP(8–37). *Acta Physiologica Scandinavica* **143**, 331–337.

GAGLIARDI M, RANDALL WC, BEIGER D, WURSTER RD, HOPKINS DA, ARMOUR JA (1988) Activity of in vivo canine cardiac plexus neurons. *American Journal of Physiology* **255**, H789–H800.

GERSTHEIMER FP, METZ J (1986) Distribution of calcitonin gene-related peptide-like immunoreactivity in the guinea-pig heart. *Anatomy & Embryology* **175**, 255–260.

GORDON L, POLAK JM, MOSCOSO GJ, SMITH A, KUHN DM, WHARTON J (1993*a*) Development of the peptidergic innervation of human heart. *Journal of Anatomy* **183**, 131–140.

GORDON L, WHARTON J, GAER JAR, INGLIS GC, TAYLOR KM, POLAK JM (1993*b*) Quantitative immunohistochemical assessment of bovine myocardial innervation before and after cryosurgical cardiac denervation. *Cardiovascular Research* **27**, 318–326.

GULBENKIAN S, WHARTON J, POLAK JM (1987) The visualisation of cardiac innervation in the guinea pig using an antiserum to PGP 9.5. *Journal of the Autonomic Nervous System* **18**, 235–247.

HAASS M, HOCK M, RICHARDT G, SCHOMIG A (1989) Neuropeptide Y differentiates between exocytotic and non-exocytotic noradrenaline release in guinea pig hearts. *Naunyn Schmiedebergs Archives of Pharmacology* **340**, 509–515.

HASSALL CJS, BURNSTOCK G (1987) Immunocytochemical localisation of neuropeptide Y and 5-hydroxytryptamine in a subpopulation of amine-handling intracardiac neurons that do not contain dopamine hydroxylase in tissue culture. *Brain Research* **422**, 74–82.

HASSALL CJS, PENKETH R, RODECK C, BURNSTOCK G (1990) The intracardiac neurons of the fetal human heart in culture. *Anatomy & Embryology* **182**, 329–337.

HILL EL, ELDE R (1989) Vasoactive intestinal peptide distribution and colocalisation with dopamine hydroxylase in sympathetic chain ganglia of pig. *Journal of the Autonomic Nervous System* **27**, 229–239.

MARRON K, WHARTON J, SHEPPARD MN, GULBENKIAN S, ROYSTON D, YACOUB MH et al. (1994) Human endocardial innervation and its relationship to the endothelium: an immunohistochemical, histochemical and quantitative study. *Cardiovascular Research* **28**, 1490–1499.

MARRON K, WHARTON J, SHEPPARD MN, FAGAN D, ROYSTON D, KUHN DM et al. (1995) Distribution, morphology, and neurochemistry of endocardial and epicardial nerve terminal arborizations in the human heart. *Circulation* **92**, 2343–2351.

MELLER ST, GEBHART GF (1992) A critical review of the afferent pathways and the potential chemical mediators involved in cardiac pain. *Neuroscience* **48**, 501–524.

MITRANI RD, ZIPES DP (1994). Clinical neurocardiology: arrhythmias. In *Neurocardiology* (ed. Armour JA, Ardell JL), pp. 365–396. New York: Oxford University Press.

MIYAZAKI T, PRIDE HP, ZIPES DP (1990) Prostaglandins in the pericardial fluid modulate neural regulation of cardiac electrophysiological properties. *Circulation Research* **66**, 163–175.

MORAVEC M, COURTALON A, MORAVEC J (1986) Intrinsic neurosecretory neurons of the rat heart atrioventricular junction: possibility of local neuromuscular feed back loops. *Journal of Molecular & Cellular Cardiology* **18**, 357–367.

MORAVEC M, MORAVEC J (1989) Adrenergic neurons and short proprioceptive feedback loops involved in the integration of cardiac function in the rat. *Cell and Tissue Research* **258**, 381–385.

MURPHY DA, O'BLENES S, HANNA BD, ARMOUR JA (1994). Capacity of intrinsic cardiac neurons to modify the acutely autotransplanted mammalian heart. *Journal of Heart & Lung Transplantion* **13**, 847–856.

RANDALL WC (1984) Selective autonomic innervation of the

heart. In *Nervous Control of Cardiovascular Function* (ed. Randall WC), pp. 46–67. New York: Oxford University Press.

RANDALL WC, THOMAS JX, BARBER MJ (1983) Selective denervation of the heart. *American Journal of Physiology* **244**, H607–H613.

RANDALL WC, ARDELL JL (1990) Nervous control of the heart: anatomy and pathophysiology. In *Cardiac Electrophysiology: From Cell to Bedside* (ed. Zipes DP, Jalife J), pp. 291–299. Philadelphia: W. B. Saunders.

SCHMOECKEL M, BHATTI FNK, ZAIDI A, COZZI E, WATERWORTH PD, TOLAN MJ et al. (1998) Orthotopic heart transplantation in a transgenic pig-to-primate model. *Transplantation* **65**, 1570–1577.

SMITH DC, PRIOLA DV (1989) Enhanced acetylcholine release from denervated atria: intrinsic neural supersensitivity. *European Journal of Pharmacology* **161**, 249–253.

SMITH FM, HOPKINS DA, ARMOUR JA (1992) Electrophysiological properties of in vitro intrinsic cardiac neurons in the pig (*Sus scrofa*). *Brain Research Bulletin* **28**, 715–725.

WHARTON J, GULBENKIAN S, MULDERRY PK, GHATEI MA, McGREGOR GP, BLOOM SR et al. (1986) Capsaicin induces a depletion of calcitonin gene-related peptide (CGRP)-like immunoreactive nerves in the cardiovascular system of the guinea pig and rat. *Journal of the Autonomic Nervous System* **16**, 289–309.

WHARTON J, POLAK JM, GORDON L, BANNER NR, SPRINGALL DR, ROSE M et al. (1990) Immunohistochemical demonstration of human cardiac innervation before and after transplantation. *Circulation Research* **66,** 900–912.

ZIPES DP, MIYAZAKI T (1990) The autonomic nervous system and the heart: basis for understanding interactions and effects on arrhythmia development. In *Cardiac Electrophysiology: From Cell to Bedside* (ed. Zipes DP, Jalife J), pp. 312–329. Philadelphia: W. B. Saunders.